Photovoltaic Array Fault Detection and Classification based on T-Distributed Stochastic Neighbor Embedding and Robust Soft Learning Vector Quantization

Shahabodin Afrasiabi, Mousa Afrasiabi, Behzad Behdani, Mohammad Mohammadi
Shiraz University
Shiraz, Iran
shpower77@yahoo.com, {musa.afra, b.behdani, m.mohammadi}@shirazu.ac.ir

Mohammad S. Javadi
INESC TEC
Porto, Portugal
msjavadi@gmail.com

Gerardo J. Osório
REMIT/UPT and C-MAST/UBI
Covilhã, Portugal
gjosilva@gmail.com

João P. S. Catalão
FEUP and INESC TEC
Porto, Portugal
catalao@fe.up.pt

2021 IEEE International Conference on Environment and Electrical Engineering and 2021 IEEE Industrial and Commercial Power Systems Europe (EEEIC / I&CPS Europe) | 978-1-6654-3613-7/21/$31.00 ©2021 IEEE | DOI: 10.1109/EEEIC/ICPSEurope51590.2021.9584770

***Abstract*—Photovoltaic (PV) as one of the most promising energy alternatives brings a set of serious challenges in the operation of the power systems including PV system protection. Accordingly, it has become even more vital to provide reliable protection for the PV generations. To this end, this paper proposes two-stage data-driven methods. In the first stage, a feature selection method, namely t-distributed stochastic neighbor embedding (t-SNE) is implemented to select the optimal features. Then, the output of t-SNE is directly fed into the strong data-driven classification algorithm, namely robust soft learning vector quantization (RSLVQ) to detect PV array fault and identify the fault types in the second stage. The proposed method is able to detect the two different line-to-line faults (in strings and out of strings) and open circuit fault and fault type considering partial shedding effects. The results have been discussed based on simulation results and have been demonstrated the high accuracy and reliability of the proposed two-stage method in detection and fault type identification based on confusion matrix values.**

Keywords—fault detection and classification, photovoltaic, robust soft learning vector quantization (RSLVQ), t-distributed stochastic neighbor embedding (t-SNE).

I. INTRODUCTION

Photovoltaic (PV) worldwide capacity has grown approximately 395:3 GW only within a decade (2007-2017) [1]. PV systems are clean, renewable, and flexible energy resources with low-level of installation and maintenance costs that are able to work both individually and cooperatively with energy storage and other power sources [2]. Hence, PV system protection is becoming more and more important. The conventional protection system of PVs might be failed due to i) the low fault current amplitudes, ii) performance of the maximum power point tracking (MPPT), iii) non-linear characteristics of the PV outputs, and iv) dependency on the meteorological information [3]. Therefore, it is essential to add a fault detection and classification method to the PV protection system. Thus, various studies have been presented to address the challenges associated with PV fault detection. The PV array fault detection methods can be divided into five main categories i.e., model-based, signal analysis-based, infrared thermography, artificial intelligence (AI)-based, and hybrid methods.

In the model-based PV array fault detection methods, firstly, the PV systems are models based on the mathematical description. Then, values obtained between the model and measurement are compared based on a predefined threshold.

J.P.S. Catalão acknowledges the support by FEDER funds through COMPETE 2020 and by Portuguese funds through FCT, under POCI-01-0145-FEDER-029803 (02/SAICT/2017). G.J. Osório acknowledges the support by UIDB/00151/2020 research unit (C-MAST) funded by FCT.

In [4], a linear Kalman filter is developed to estimate the PV model parameters to detect abnormal conditions. Also, least-square (LS) based fault detection for PV arrays is presented in [5]. Although model-based methods perform fast, accurate mathematical modeling of the nonlinear characteristics of PV systems with several components is too difficult. Moreover, the model-based methods are highly dependent on the predefined threshold [6].

Signal processing methods utilized time-domain or frequency-domain analysis techniques to extract features for discrimination between the normal and abnormal conditions. For instance, the Teager-Kaiser energy operator as a signal-processing measure is presented in [7] to detect line-to-line faults. In [8], wavelet-transform as a spectral analysis technique is used to detect the fault based on the measured voltage, voltage energy, and impedance variations. Signal-processing-based fault detection methods do not depend on the physical model, however, these methods still depend on the predefined threshold and are highly sensitive to external disturbances such as noise [9].

The fault occurrence in PV arrays can cause thermal imbalance due to the formation of hot spots. Therefore, fault occurrence leads to the temperature increasing in the PV modules. Thus, by monitoring the temperature, the fault event can be detected. To this end, infrared thermography is a typical tool to monitor PV systems, which performs based on the conversion of the PV temperature into a set of images [3]. Using infrared thermography for fault detection is a highly accurate method for fault detection. However, it is very expensive for PV monitoring and also requires additional manpower to monitor a large number of PV modules in large-scale PV systems.

AI-based methods perform only based on historical data. Firstly, a machine learning structure is trained based on the historical data and, then perform as an expert-smart box to monitor the system [10]. With the emergence of new technologies, the cost of AI-based methods is significantly reduced. The AI-based methods are a potential candidate to handle the complexities associated with the problem of fault detection in PV arrays [11].

To this end, several AI-based methods have been presented in recent years for PV system monitoring. The k-nearest neighbor (kNN) [12], extreme learning machine (ELM) [13], decision tree (DT) [14], support vector machine (SVM) [15], and random forest (RF) [16] are several examples of AI-based methods for the PV monitoring system. However, AI-based methods generally perform poorly based on the raw data due to the small number of the parameter [17].

978-1-6654-3613-7/21/$31.00 ©2021 IEEE

Thus, a feature engineering technique is required for accurate performance. The fault detection methods based on AI-based structure are not solely capable of learning and being properly trained the complex and varying behaviors reflected by the signal datasets. The majority of the present AI-based methodologies are presented based on the feature extraction techniques such as wavelet transform combination with artificial neural network (ANN) [18] and empirical mode decomposition (EMD combined with SVM in [19]. However, these techniques are highly noise-sensitive and might increase information redundancy [20].

In this paper, this problem has been tackled by conducting the feature selection method, namely t-distribution stochastic neighbor embedding (t-SNE) to select the optimal features based on raw data. Then a robust soft learning vector quantization (RSLVQ), as an enhanced probabilistic version of the simple LVQ is developed to detect and classify the PV array faults. The LVQ is a supervised artificial neural network and can realize based on a codebook vector collection, being able to handle both binary and multiclass diagnosis problems. RSLVQ deals with the problem of LVQ to minimize the classification error through a solely heuristic process. The proposed hybrid intelligent method.

Thus, the contributions of the paper can be summarized as:

- A strong nonlinear feature selection technique is used to separate the high importance features in the PV fault diagnosis and classification
- A probabilistic LVQ structure is developed to accurately detect and classify the faults

The rest of the paper is organized as follows: Section II described the hybrid method. The numerical results are discussed in Section III. The study is concluded in Section IV.

II. Proposed Method

PV fault detection and type determination based on the proposed scheme are carried out in two steps. The primary step constitutes the utilization of a feature extractor developed based on t-SNE. This step extracts the features of the measured signals, helping a better distinction of faults. Subsequently, these features are used in the powerful RSLVQ classifier to first discriminate between the faulty and non-faulty conditions, and then between different types of PV faults. The following subsections provide a more detailed explanation of these two successive steps.

A. The t-SNE feature extractor

The t-SNE can be described as an unsupervised, yet powerful nonlinear tool for feature extraction, which in the simplest terms, operates based on the similarity between two large-dimension datasets. In this method, the probability density between two sets with large and small dimensions is put into application to determine the highest similarity. This end is attained by using the Kullback Leibler (KL) divergence to develop an objective function in the computations. The following belongs to the implementation of the t-SNE method. Assuming that the different elements in the dataset are as $\{x_1, x_2, \ldots, x_N\}$; the similarity probability of two points is as:

$$p_{i|j} = \frac{\exp\left(\frac{-\| x_j - x_i \|^2}{2\sigma_j}\right)}{\sum_{k=1,k\neq j}^{N} \exp\left(\frac{-\| x_j - x_k \|^2}{2\sigma_j}\right)} \quad (1)$$

$$p_{j|i} = \frac{\exp\left(\frac{-\| x_i - x_j \|^2}{2\sigma_i}\right)}{\sum_{k=1,k\neq i}^{N} \exp\left(\frac{-\| x_i - x_k \|^2}{2\sigma_i}\right)} \quad (2)$$

where the likelihood between two different elements of the dataset is characterized by $p_{i|j}$ and $p_{j|i}$, and σ_j is the variance vector of the Gaussian distribution with j being the center point. Accordingly, the joint probability of two samples within a Gaussian space is yielded as:

$$p_{ij} = \frac{p_{i|j} + p_{j|i}}{2N} \quad (3)$$

Since the t probability distribution with one degree of freedom is applied for lower dimensions, the q_{ij} joint PDFs of the dataset elements belonging to the set $\{y_1, y_2, \ldots, y_N\}$ is:

$$q_{ij} = \frac{\left(1+\| y_i - y_j \|^2\right)^{-1}}{\sum_{k=1,k\neq l}^{N} \left(1+\| y_k - y_l \|^2\right)^{-1}} \quad (4)$$

Using KL divergence to determine the similarity between q_{ij} and p_{ij}, the following is obtained:

$$C = KL\left(P \| Q\right) = \sum_{i=1}^{N}\sum_{j=1}^{N} p_{ij} \log_2 \frac{p_{ij}}{q_{ij}} \quad (5)$$

For maximization of the similarity, the KL divergence index must be minimum. Therefore, with the help of the gradient descent optimization, the following is achieved as:

$$\frac{\delta C}{\sigma y_i} = 4\sum_{j=1}^{N}\left(p_{ij} - q_{ij}\right)\left(y_j - y_i\right)\left(1+\| y_i - y_j \|^2\right)^{-1} \quad (6)$$

Accordingly, the set of features as $\{y_1', y_2', \ldots, y_N'\}$ is determined by the t-SNE based on the raw measurements of the PV panel.

B. The RSLVQ classifier

In order to enhance the capabilities of LVQ, taking heuristic grounds into consideration, a modified version, i.e., a probabilistic robust soft LVQ was introduced [21]. The original LVQ is inherently a powerful classifier that operates very well with small dimension datasets and can be also matched together with other AI-based algorithms, proving its superior performance among different classifier tools [21]-[23]. On this account, RSLVQ being an enhanced version of LVQ, one can expect to obtain a very high classification performance by using RSLVQ.

In RSLVQ, the classes are first labeled with “correct” and “incorrect” and assumed with Gaussian mixture probability density functions (PDFs). Subsequently, a cost-function is developed based on the logarithm of the ratio of “correct” over “incorrect” PDFs. This provides two logarithmic probability terms, each corresponding to the classes “correct” and “incorrect.”

Here, a cost function according to [22] was considered for the RSLVQ which is defined as follows:

$$f_{RSLVQ} = \prod_{k=1}^{N} \frac{P(X_k, Y_k \setminus \Gamma)}{P(X_k, Y_k \setminus \Gamma) + P(X_k, Y_k^{'} \setminus \Gamma)} = \prod_{k=1}^{N} \frac{P(X_k, Y_k \setminus \Gamma)}{P(X_k \setminus \Gamma)} \quad (6)$$

where N corresponds to the total number of samples. Also, the sets X_k and $Y = \{c_j, c_{In}\}$ are defined as the set of inputs and the set of labels, respectively. The dataset for non-faulty signals is denoted by c_j while c_{In} will correspond to the faulty signals in the case of fault detection, and it will correspond to the dataset of different fault types in the case of fault type discrimination. The nearest prototype classifier is defined as $\Gamma = \{(L_{f/In}, c_{f/In})\}$ to comprise the data space vectors, i.e., non-faulty together with faulty signals and the dataset of fault types, and the labels of their corresponding classes. This choice of the cost function in (7) helps maximize the rate of correct classifications and also minimize the incorrect classifications at the same time. The defined cost function is always bounded to the interval of 0 to 1, and thus, we have:

$$\log(f_{RSLVQ}) = \sum_{k=1}^{N} \log \frac{P(X_k, Y_k \setminus \Gamma)}{P(X_k, Y_k^{'} \setminus \Gamma)} \quad (8)$$

Employing the stochastic gradient ascent for updating the learning rule, the following is obtained as:

$$L_{f/In}(t+1) = L_{f/In}(t) + \alpha(t) \frac{\partial}{\partial L_{f/In}} \{\log \frac{P(X, Y \setminus \Gamma)}{P(X \setminus \Gamma)}\} \quad (9)$$

where the learning rate is characterized by α(t). Accordingly, the learning rule is calculated from the gradient:

$$L_{f/In}(t+1) = L_{f/In}(t) + \alpha(t) \begin{cases} (P_Y(l \setminus X) - P(l \setminus X)[\frac{\partial f(X, L_{f/In})}{\partial L_{f/In}}] & , c_l = Y \\ -P(l \setminus X)[\frac{\partial f(X, L_{f/In})}{\partial L_{f/In}}] & , c_l \neq Y \end{cases} \quad (10)$$

where the probabilities PY(l\X) and P(l\X) describe the probability of X to be assigned to the component 1 of the mixture respective to the class of correctly classified samples and all other classes as:

$$P_Y(l \setminus X) = \frac{P(l) \exp f(X, L_{f/In})}{\sum_{\{j:c_{j=Y}\}} P(j) \exp f(X, L_{f/In,j})} \quad (11)$$

$$P(l \setminus X) = \frac{P(l) \exp f(X, L_{f/In})}{\sum_{j=1}^{2} P(j) \exp f(X, L_{f/In,j})} \quad (12)$$

By adopting a Gaussian mixture model for components with the same widths and strengths in conditional probabilities, the following yields:

$$f(X, L_{f/In}) = \frac{-(x - L_{f/In})^2}{2\sigma^2} \quad (13)$$

$$\frac{\partial}{\partial L_{f/In}} f(X, L_{f/In}) = \frac{(x - L_{f/In})}{\sigma^2} \quad (14)$$

$$P_Y(l \setminus X) = \frac{\exp(\frac{-(x - L_{f/In})^2}{2\sigma^2})}{\sum_{\{j:c_{j=Y}\}} \exp(\frac{-(x - L_{f/In})^2}{2\sigma^2})} \quad (15)$$

$$P(l \setminus X) = \frac{\exp(\frac{-(x - L_{f/In})^2}{2\sigma^2})}{\sum_{j=1}^{M} \exp(\frac{-(x - L_{f/In})^2}{2\sigma^2})} \quad (16)$$

Finally, the learning rule is obtained as:

$$L_{f/In}(t+1) = L_{f/In}(t) + \frac{\alpha(t)}{2\sigma^2} \begin{cases} (P_Y(l \setminus X) - P(l \setminus X)(X - L_{f/In}) & , c_l = Y \\ -P(l \setminus X)(X - L_{f/In}) & , c_l \neq Y \end{cases} \quad (17)$$

where a positive constant, σ, is defined to describe the softness factor.

III. Numerical Results

The test system demonstrated in Fig. 1 is selected for implementation of the proposed scheme. This test system is a radial distribution network with a voltage level of 25 kV, fed from an upper-hand grid with a short-circuit capacity of 2500 MVA. A 250 kV PV system constituted of 10 series panels, and a boost-type DC-DC converter, forming a voltage source converter (VSC) unit is included in the network. MATLAB/Simulink environment is used for simulating the test system and generating the dataset.

The dataset required for training is generated by considering different operating and fault conditions in the system under study. The specifications given in Table I describe the various parameters considered for solar radiation, ambient temperature, and fault resistance. Five different fault configurations F1, F2, F3, F4, and F5 are considered in this study as shown in Fig. 2. Various combinations of faults between poles of same and different strings are including for the sake of forming a comprehensive dataset.

TABLE I. Specifications For Dataset Generation

Parameter	Value
Solar Radiation	700-1000 [W/m^2]
Temperature	5, 20, 24, 25, 45 [°C]
Fault Resistance	0, 0.001, 0.01, 16 [Ω]

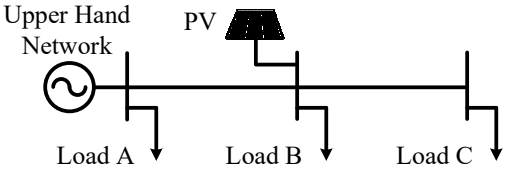

Fig. 1: Test system adopted for the implementation of the proposed scheme.

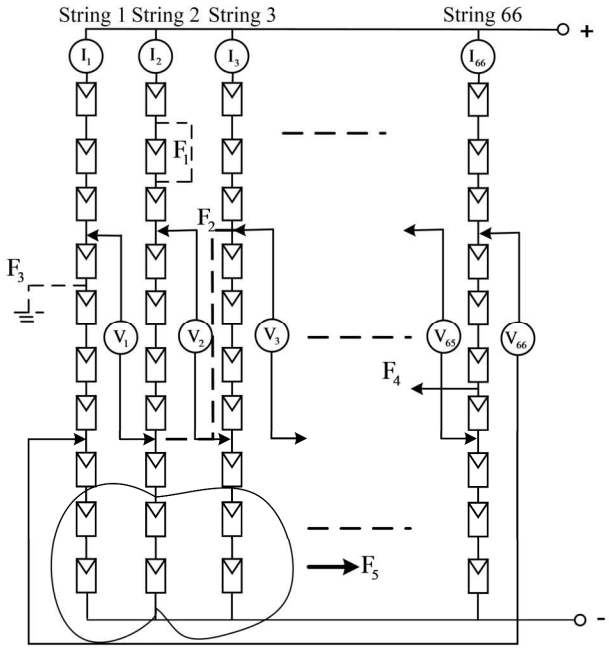

Fig. 2: Different PV fault configurations considered.

The fault detection and classification in this method is carried out by employing a window-length of 100 samples. Moreover, the cosine distance criterion is applied for feature extraction in the t-SNE classifier. In the following, the performance of the proposed scheme is discussed.

A. t-SNE Feature Extractor Performance

In the first stage, the fault dataset generated based on the specifications described in Table I, and the various fault configurations shown in Fig. 2 is utilized as the input to the t-SNE feature extractor. Primarily, t-SNE is used for fault detection. The performance of t-SNE in discriminating between normal (class 0) and faulty conditions (class 1) using voltage signal inputs and based on cosine distance criterion is shown in Fig. 3. As can be seen, t-SNE is confirmed to be an appropriate feature selection method for PV fault identification.

TABLE III. CONFUSION MATRIX OBTAINED BY THE POPOSED HYBRID METHOD FOR PV FAULT DETECTION

CLASSES	0'	1'	SUM
0	234	0	234
1	0	243	243
Total Samples	234	243	477

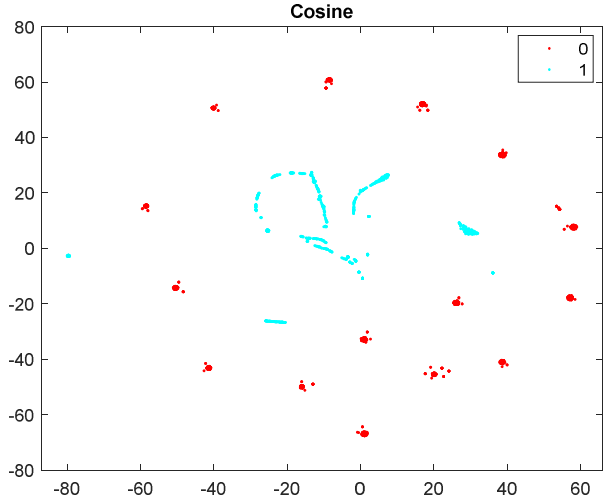

Fig. 3: t-SNE results on fault detection.

TABLE II. COFUSION MATRIX OBTAINED BY THE POPOSED HYBRID METHOD FOR PV FAULT TYPE IDENTIFICATION

CLASSES	1'	2'	3'	4'	SUM
1	547	0	0	0	547
2	0	223	32	0	232
3	0	17	260	0	26
4	0	0	0	34	34
Total Sample	547	240	292	34	1113

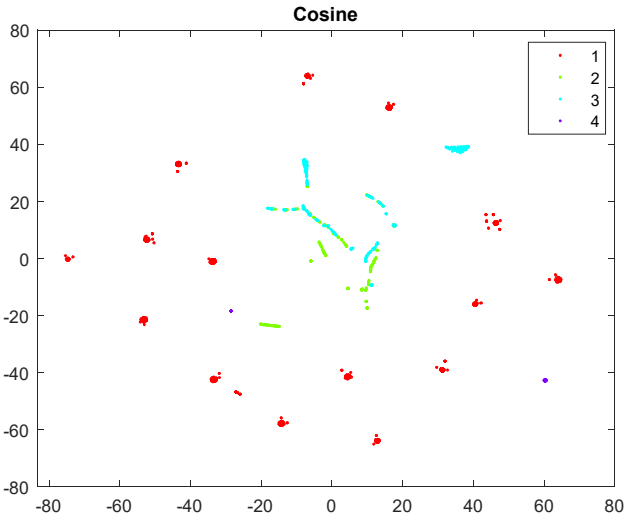

Fig. 4: t-SNE results on fault type determination.

Afterward, the fault dataset is processed by the t-SNE feature extractor to determine fault types. Similarly, voltage signals are used and cosine distance criterion is applied. As shown in Fig. 4, the acceptable ability of t-SNE in fault type determination is verified. It is worth noting that the fault types considered are consisting of in-string (class 1), out-string (class 2), open-circuit (class 3), together with the normal condition without fault (class 4).

B. RSLVQ Classifier Performance

In the second stage, to evaluate the performance of the proposed RSLVQ classifier for fault detection and fault type determination, the confusion matrix criterion is applied. The confusion matrixes are defined based on four main members given by true-positive (TP): cases that belong to a certain and are correctly classified; false-positive (FP): cases that do not belong to a certain class but are mistakenly included in that class; true-negative (TN): cases which do not belong to a certain class and are correctly not included in that class; and false-negative (FN): cases which belong to a certain class but are mistakenly not included in that class. The confusion matrixes for the RSLVQ's performance in fault detection and fault type identification are demonstrated in Tables II and III, respectively.

IV. CONCLUSION

In this study, a two-stage PV fault detection and type identification approach is proposed based on t-SNE and RSLVQ. Employing the measured voltage signals, a t-SNE feature extractor is used in the first stage. The cosine distance

criterion was used for a better distinction of features. Afterward, an RSLVQ network is utilized as a classifier, making use of the features extracted by t-SNE. A test radial distribution system integrated with a PV unit was applied to implement and test the proposed scheme. Considering various fault configurations, a comprehensive dataset was gathered and then fed to the proposed method. The results obtained from the t-SNE show the capability of the proposed feature extractor to distinct classes of faulty and non-faulty conditions, and also classes of different fault types. Furthermore, the excellent performance of the RSLVQ classifier is demonstrated by the confusion matrixes for fault detection and fault type determination. Therefore, the proposed method is verified to be a suitable method for PV fault detection and type identification.

REFERENCES

[1] M. Afrasiabi, M. Mohammadi, M. Rastegar, and S. Afrasiabi, "Deep learning architecture for direct probability density prediction of small-scale solar generation," IET Generation, Transmission & Distribution, vol. 14, no. 11, pp. 2017-2025, Apr. 2020, doi: doi.org/10.1049/iet-gtd.2019.1289.

[2] M. Afrasiabi, M. Mohammadi, M. Rastegar, and A. Kargarian, "Multi-agent microgrid energy management based on deep learning forecaster," Energy, vol. 186, p. 115873, Jan. 2019, doi: 10.1016/j.energy.2019.115873.

[3] D. S. Pillai and N. Rajasekar, "A comprehensive review on protection challenges and fault diagnosis in PV systems," Renewable and Sustainable Energy Reviews, vol. 91, pp. 18-40, Aug. 2018, doi: 10.1016/j.rser.2018.03.082.

[4] T. Ghanbari and S. R. K. Hoseini, "KF-based technique for detection of anomalous condition of the PV panels," IET Generation, Transmission & Distribution, vol. 10, no. 15, pp. 3698-3706, Nov. 2016, doi: 10.1049/iet-gtd.2015.1514.

[5] T. Andrianajaina, E. J. R. Sambatra, C. Bernard Andrianirina, T. David Razafimahefa and N. Heraud, "PV fault detection using the least squares method," 2016 International Conference and Exposition on Electrical and Power Engineering (EPE), 2016, pp. 846-851, doi: 10.1109/ICEPE.2016.7781456.

[6] S. Afrasiabi, M. Mohammadi, M. Afrasiabi, and B. Parang, "Modulated Gabor filter based deep convolutional network for electrical motor bearing fault classification and diagnosis," IET Science, Measurement & Technology, vol. 15, no. 2, pp. 154-162, Jan. 2021, doi: 10.1049/smt2.12017.

[7] A. Khoshnami and I. Sadeghkhani, "Fault detection for PV systems using Teager–Kaiser energy operator," Electronics Letters, vol. 54, no. 23, pp. 1342-1344, Nov. 2018, doi: 10.1049/el.2018.6510.

[8] B. P. Kumar, G. S. Ilango, M. J. B. Reddy and N. Chilakapati, "Online Fault Detection and Diagnosis in Photovoltaic Systems Using Wavelet Packets," in IEEE Journal of Photovoltaics, vol. 8, no. 1, pp. 257-265, Jan. 2018, doi: 10.1109/JPHOTOV.2017.2770159.

[9] S. Afrasiabi, M. Afrasiabi, B. Parang, M. Mohammadi, S. Kahourzade and A. Mahmoudi, "Two-Stage Deep Learning-based Wind Turbine Condition Monitoring Using SCADA Data," 2020 IEEE International Conference on Power Electronics, Drives and Energy Systems (PEDES), 2020, pp. 1-6, doi: 10.1109/PEDES49360.2020.9379393.

[10] S. Afrasiabi, M. Afrasiabi, B. Parang and M. Mohammadi, "Integration of Accelerated Deep Neural Network Into Power Transformer Differential Protection," in IEEE Transactions on Industrial Informatics, vol. 16, no. 2, pp. 865-876, Feb. 2020, doi: 10.1109/TII.2019.2929744.

[11] S. Afrasiabi, M. Afrasiabi, M. Mohammadi, and B. Parang, "Fault localisation and diagnosis in transmission networks based on robust deep Gabor convolutional neural network and PMU measurements," IET Generation, Transmission & Distribution, vol. 14, no. 26, pp. 6484-6492, Dec. 2020, doi: 10.1049/iet-gtd.2020.0856.

[12] F. Harrou, B. Taghezouit and Y. Sun, "Improved kNN-Based Monitoring Schemes for Detecting Faults in PV Systems," in IEEE Journal of Photovoltaics, vol. 9, no. 3, pp. 811-821, May 2019, doi: 10.1109/JPHOTOV.2019.2896652.

[13] V. Le, X. Yao, C. Miller and B. Tsao, "Series DC Arc Fault Detection Based on Ensemble Machine Learning," in IEEE Transactions on Power Electronics, vol. 35, no. 8, pp. 7826-7839, Aug. 2020, doi: 10.1109/TPEL.2020.2969561.

[14] R. Benkercha and S. Moulahoum, "Fault detection and diagnosis based on C4.5 decision tree algorithm for grid connected PV system," Solar Energy, vol. 173, pp. 610-634, Oct. 2018, doi: 10.1016/j.solener.2018.07.089.

[15] Zhehan Yi and A. H. Etemadi, "A novel detection algorithm for Line-to-Line faults in Photovoltaic (PV) arrays based on support vector machine (SVM)," 2016 IEEE Power and Energy Society General Meeting (PESGM), 2016, pp. 1-4, doi: 10.1109/PESGM.2016.7742026.

[16] Z. Chen et al., "Random forest based intelligent fault diagnosis for PV arrays using array voltage and string currents," Energy Conversion and Management, vol. 178, pp. 250-264, Dec. 2018, doi: 10.1016/j.enconman.2018.10.040.

[17] H. Samet, S. Ketabipour, M. Afrasiabi, S. Afrasiabi and M. Mohammadi, "Deep Learning Forecaster based Controller for SVC: Wind Farm Flicker Mitigation," in IEEE Transactions on Industrial Informatics, doi: 10.1109/TII.2020.3025101.

[18] I. M. Karmacharya and R. Gokaraju, "Fault Location in Ungrounded Photovoltaic System Using Wavelets and ANN," in IEEE Transactions on Power Delivery, vol. 33, no. 2, pp. 549-559, April 2018, doi: 10.1109/TPWRD.2017.2721903.

[19] W. Miao, Q. Xu, K. H. Lam, P. W. T. Pong and H. V. Poor, "DC Arc-Fault Detection Based on Empirical Mode Decomposition of Arc Signatures and Support Vector Machine," in IEEE Sensors Journal, vol. 21, no. 5, pp. 7024-7033, 1 March1, 2021, doi: 10.1109/JSEN.2020.3041737.

[20] S. Afrasiabi, M. Afrasiabi, B. Parang, M. Mohammadi, M. M. Arefi and M. Rastegar, "Wind Turbine Fault Diagnosis with Generative-Temporal Convolutional Neural Network," 2019 IEEE International Conference on Environment and Electrical Engineering and 2019 IEEE Industrial and Commercial Power Systems Europe (EEEIC / I&CPS Europe), 2019, pp. 1-5, doi: 10.1109/EEEIC.2019.8783233.

[21] S. Seo and K. Obermayer, "Soft Learning Vector Quantization," *Neural Comput.*, vol. 15, no. 7, pp. 1589–1604, Jul. 2003, doi: 10.1162/089976603321891819.

[22] T. Villmann, M. Biehl, A. Villmann and S. Saralajew, "Fusion of deep learning architectures, multilayer feedforward networks and learning vector quantizers for deep classification learning," 2017 12th International Workshop on Self-Organizing Maps and Learning Vector Quantization, Clustering and Data Visualization (WSOM), 2017, pp. 1-8, doi: 10.1109/WSOM.2017.8020009.

[23] D. Hofmann, A. Gisbrecht, and B. Hammer, "Efficient approximations of robust soft learning vector quantization for non-vectorial data," *Neurocomputing*, vol. 147, pp. 96–106, Jan. 2015, doi: 10.1016/j.neucom.2013.11.044.